

Structural Biological Composites: An Overview*

Marc A. Meyers, Albert Y.M. Lin, Yasuaki Seki, Po-Yu Chen, Bimal K. Kad, and Sara Bodde

Biological materials are complex composites that are hierarchically structured and multifunctional. Their mechanical properties are often outstanding, considering the weak constituents from which they are assembled. They are for the most part composed of brittle (often, mineral) and ductile (organic) components. These complex structures, which have risen from millions of years of evolution, are inspiring materials scientists in the design of novel materials. This paper discusses the overall design principles in biological structural composites and illustrates them for five examples: sea spicules, the abalone shell, the conch shell, the toucan and hornbill beaks, and the sheep crab exoskeleton.

INTRODUCTION

Many biological systems have mechanical properties that are far beyond those that can be achieved using the same synthetic materials with present technologies.¹ This is because biological organisms produce composites that are organized in terms of composition and structure, containing both inorganic and organic components in complex structures. They are hierarchically organized at the nano-, micro-, and meso-levels. Additionally, most biological materials

are multifunctional² (i.e., they accumulate functions). For example, bone provides structural support for the body plus blood cell formation; the chitin-based exoskeleton in arthropods offers an attachment for muscles, environmental protection, and a water barrier; sea spicules offer light transmission plus structural support; and roots anchor trees plus provide nutrient transport. A third defining characteristic of biological systems, in contrast with current synthetic systems, is their self-healing ability. This is nearly universal in nature. Although biology is a mature science, the study of biological materials and systems by materials scientists and engineers is recent. It is intended, ultimately, to accomplish two purposes. First, this study provides the tools for the development of biologically inspired materials. This field, also called biomimetics,³ is attracting increasing attention and is one of the new frontiers in materials research. Second, the study of biological materials enhances the understanding of the interaction of synthetic materials and biological structures with the goal of enabling the introduction of new and complex systems in the human body, leading eventually to organ supplementation and substitution. These are the

so-called biomaterials.

One of the defining features of the rigid biological systems that comprise a significant fraction of the structural biological materials is the existence of two components: a mineral and an organic component. The intercalation of these components can occur at the nano-, micro-, or meso-scale and often takes place at more than one dimensional scale. Table I exemplifies this for a number of systems. The mineral component provides the strength whereas the organic component contributes to the ductility. This combination of strength and ductility leads to high energy absorption prior to failure. The most common mineral components are calcium carbonate, calcium phosphate (hydroxyapatite), and amorphous silica, although more than 20 minerals, with principal elements being Ca, Mg, Si, Fe, Mn, P, S, C, and the light elements H and O. These minerals are embedded in a complex assemblage of organic macromolecules⁴ that are hierarchically organized. The best known are keratin, collagen, and chitin.

The extent and complexity of the subject are daunting and will require many years of global research effort to be elucidated. Thus, the focus here is on five systems that have attracted the interest

Table I. Principal Components of Common Structural Biological Composites

Biological Composite	Mineral					Organic				
	Calcium Carbonate	Calcium	Silica	Hydroxyl Apatite	Other	Keratin	Collagen	Chitin	Cellulose	Other
Shells	X									X
Horns		X				X				
Bones				X			X			
Teeth				X						X
Bird Beaks		X				X				
Crustacean Exoskeleton	X							X		X
Insect Cuticle								X		X
Woods									X	
Spicules			X							X

of the authors. The silica spicules have been studied and extensively described by Mayer and coworkers.^{5,6} The four other systems have been investigated by the authors: abalone,⁷⁻⁹ conch,^{9,10} toucan,^{11,12} and crab exoskeleton.¹³

HIERARCHICAL ORGANIZATION OF STRUCTURE

It could be argued that all materials are hierarchically structured, since the changes in dimensional scale bring about different mechanisms of deformation and damage. However, in biological materials this hierarchical organization is inherent to the design. The design of the material and structure are intimately connected in biological systems, whereas in synthetic materials there is a disciplinary separation, based largely on tradition, between materials (materials engineers) and structures (mechanical engineers). This is illustrated by three examples in Figure 1 (bone), Figure 2 (abalone shell), and Figure 3 (crab exoskeleton).

In bone (Figure 1), the building block of the organic component is the collagen, which is a triple helix with a diameter of approximately 1.5 nm. These tropocollagen molecules are intercalated with the mineral phase (hydroxyapatite, a calcium phosphate) forming fibrils that, on their turn, curl into helicoids of alternating directions. These osteons are the basic building blocks of bones. The weight fraction distribution between the organic and mineral phase is approximately 60/40, making bone unquestionably a complex hierarchically structured biological composite.

Similarly, the abalone shell (Figure 2) owes its extraordinary mechanical properties (much superior to monolithic CaCO_3) to a hierarchically organized structure, starting at the nano-level, with an organic layer having a thickness of 20–30 nm, proceeding with single crystals of the aragonite polymorph of CaCO_3 , consisting of “bricks” with dimensions of 0.5 μm vs. 10 μm (microstructure), and finishing with layers approximately 0.3 mm (mesostructure).

Crabs are arthropods whose carapace comprises a mineralized hard component, which exhibits brittle fracture, and a softer, organic component, which is primarily chitin. These two components are shown in the scanning-electron

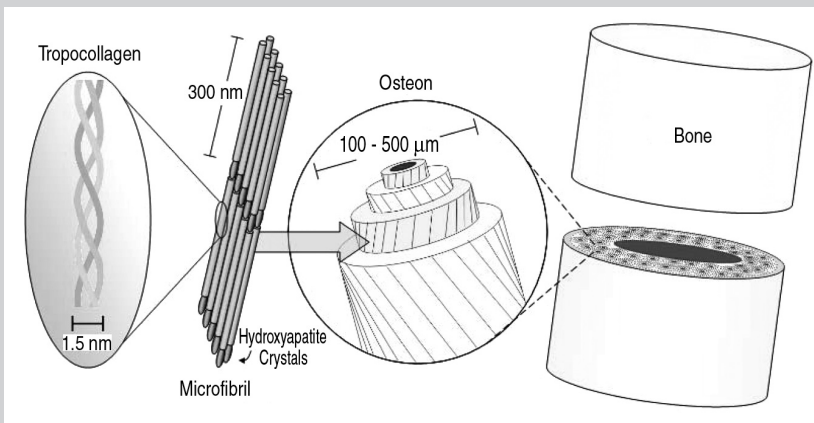


Figure 1. The hierarchical organization of bone.

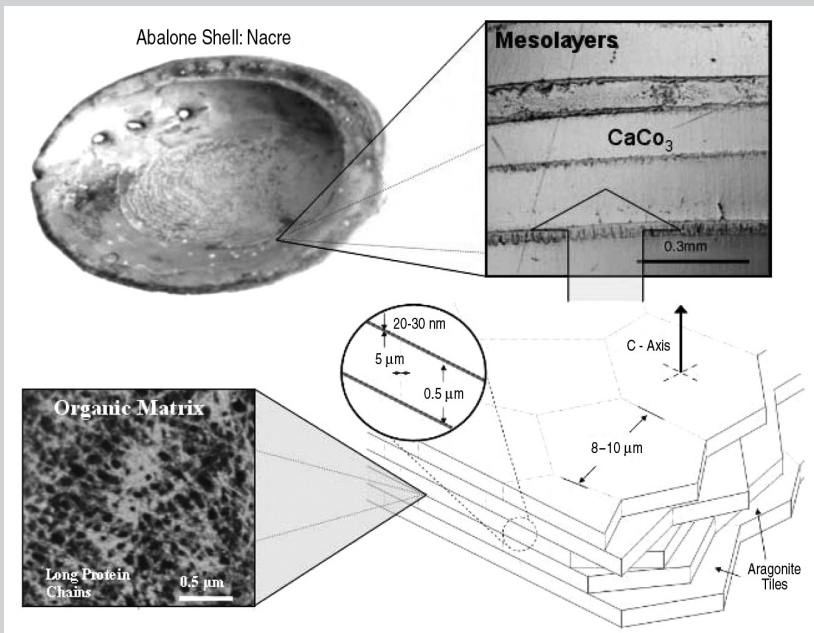


Figure 2. The hierarchy of abalone structure. Clockwise from top left: entire shell; mesostructure with mesolayers; microstructure with aragonite tiles; nanostructure showing organic interlayer comprising 5 wt.% of overall shell.

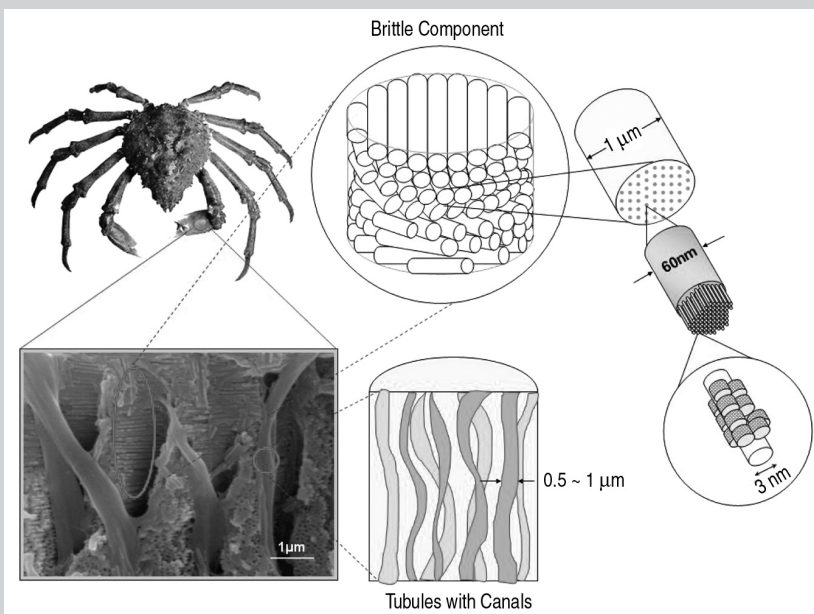


Figure 3. The hierarchy of spider crab structure.

micrograph (SEM) of Figure 3. The brittle component is arranged in a helical pattern called a Bouligand structure. There are canals linking the inside to the outside of the shell; they are bound by tubules shown in the micrograph and in a schematic fashion. The hard mineralized component has darker spots seen in

the SEM. At higher magnification, this consists of a chitin-protein mixture.

SPONGE SPICULES

Sea sponges have often long rods that protrude out. Their outstanding flexural toughness was first discovered by Levi et al.,¹⁴ who were able to bend a 1 m rod,

having a diameter similar to a pencil, into a full circle. This deformation was fully reversible. Additionally, these rods are multifunctional and carry light. The optical properties were studied by Aizenberg et al.¹⁵ Figure 4 shows a fractured hexactinellid spicule (much smaller than the one studied by Levi et al.¹⁴) that reveals its structure. This spicule, which has been studied by Mayer and Sarikaya,¹⁶ is a cylindrical amorphous silica rod and has an onion-skin type structure which effectively arrests cracks and provides an increased flexural strength. Figure 4b shows the flexural stress as a function of strain. The spicule response is compared with that of a synthetic monolithic silica rod. The breaking stress of the spicule is four times higher than the monolithic silica. Additionally, an important difference exists between the two: whereas the monolithic silica breaks in a single catastrophic event, the spicule breaks gracefully with progressive load drops. This is the direct result of the arrest of the fracture at the onion layers. These intersilica layers contain an organic component which has been identified by Cha, Morse, and coworkers¹⁷ as silicatein (meaning a silica-based protein).

NACREOUS SHELLS

The growth and self-assembly of aragonitic calcium carbonate found in many shells is a fascinating and still not completely understood process. The deposition of a protein layer of approximately 20–30 nm is intercalated with aragonite platelets, which are remarkably constant in dimension for each animal. In the case of the abalone shell, the mineral phase corresponds to approximately 95% of the total volume. This platelet size was found to be constant for abalone shells with varying diameters of 10 mm, 50 mm, and 200 mm.⁸ However, there are differences between species: the thickness of the tiles in the abalone shells is approximately 0.5 μm, as seen in Figure 5a, while it is around 1.5 μm for a bivalve shell found in the Araguaia River (Brazil), thousands of miles from the ocean (Figure 5b). Periodic growth arrests create mesolayers¹ that play a critical role in the mechanical properties and are powerful crack deflectors. These mesolayers are separated by a thicker viscoelastic organic layer that is interspersed with the mineral phase.

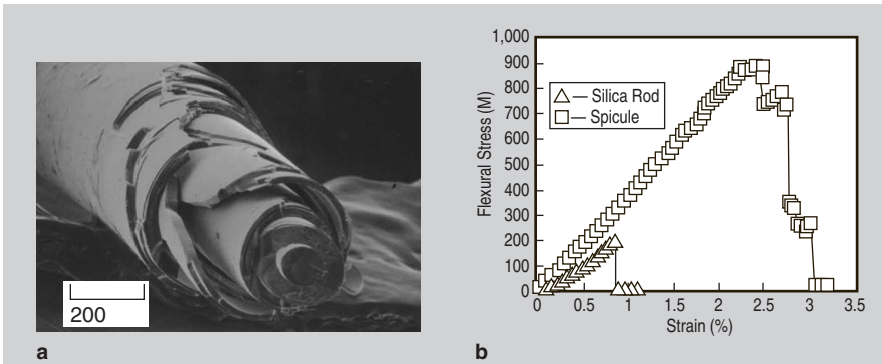


Figure 4. (a) A fractured spicule on sea sponge; (b) flexural stress vs. strain for monolithic (synthetic) and for sea spicule (Courtesy of G. Mayer, University of Washington).

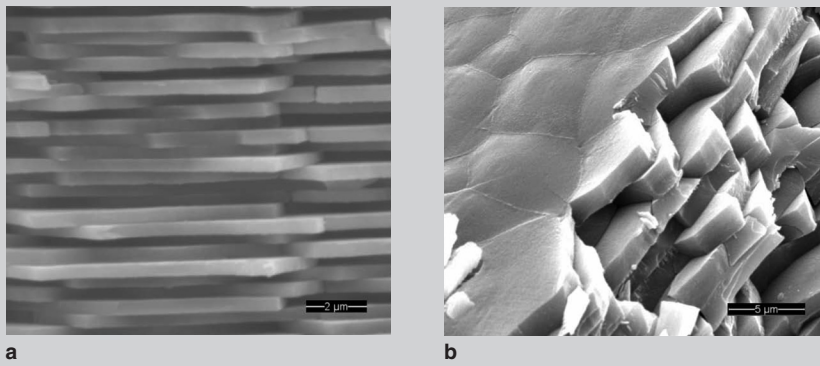


Figure 5. Nacreous tile structures; (a) abalone (*Haliotis rufescens*) from Southern California; (b) bivalve shell from Araguaia River, Brazil.

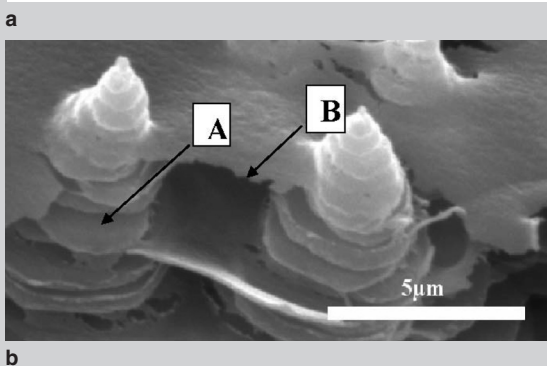
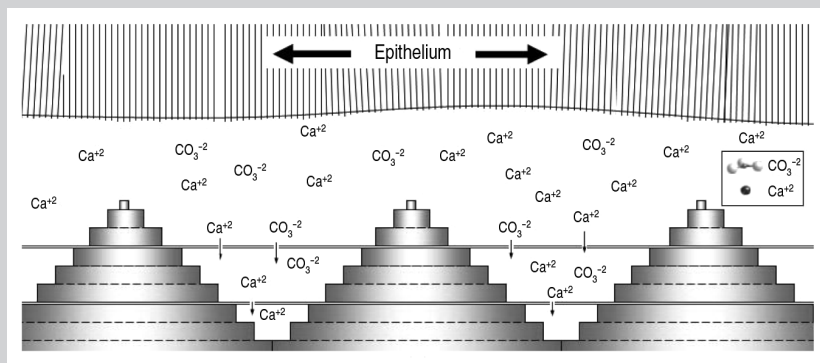


Figure 6. The growth of nacreous tiles by terraced cone mechanism. (a) A schematic of growth mechanism showing intercalation of mineral and organic layers; (b) SEM of arrested growth showing partially grown tiles (arrow A) and organic layer (arrow B).

The growth of the aragonite component of the composite occurs by the successive arrest of growth by means of a protein-mediated mechanism; this is followed by the reinitiation of growth. This takes place in the Christmas-tree pattern and is represented in Figure 6a. The calcium and carbonate ions can penetrate through the organic layer deposited by the epithelium. The growth of the nacreous layers (aragonite) was observed by Lin and Meyers⁸ inserting glass plates in the extrapallial layer for different time periods, removing them, and observing them by SEM. Details of the growth sequence were revealed.

Quasi-static and dynamic compression and three-point bending tests were carried out by Menig et al.⁷ The mechanical response was found to vary significantly from specimen to specimen and required the application of Weibull statistics in order to be quantitatively evaluated. The abalone exhibited orientation dependence of strength as well as significant strain-rate sensitivity; the failure strength at loading rates of 10^4 GPa/s was approximately 50% higher than the quasi-static strength. The abalone compressive strength when loaded perpendicular to the shell surface was approximately 50% higher than parallel to the shell surface. Quasi-static compressive failure in both shells occurred gradually, in graceful failure. The shear strength of the organic/ceramic interfaces of *Haliotis rufescens* was determined by means of a shear test and was found to be approximately 30 MPa. Considerable inelastic deformation of these layers (up to a shear strain of 0.4) preceded failure. Crack deflection, delocalization of damage, plastic microbuckling (kinking), and viscoplastic deformation of the organic layers are the most important mechanisms contributing to the unique mechanical properties of these shells. Figure 7a shows the tensile failure along the direction of the tiles. The tensile strength of the tiles is such that they do not in general break, but slide. The tile sliding represented in Figure 7b. This is accomplished by the viscoplastic deformation of the organic layer and/or by the shearing of the mineral ligaments traversing the organic phase. Upon compression perpendicular to the plane of the tiles, an interesting phenomenon observed previously in composites was

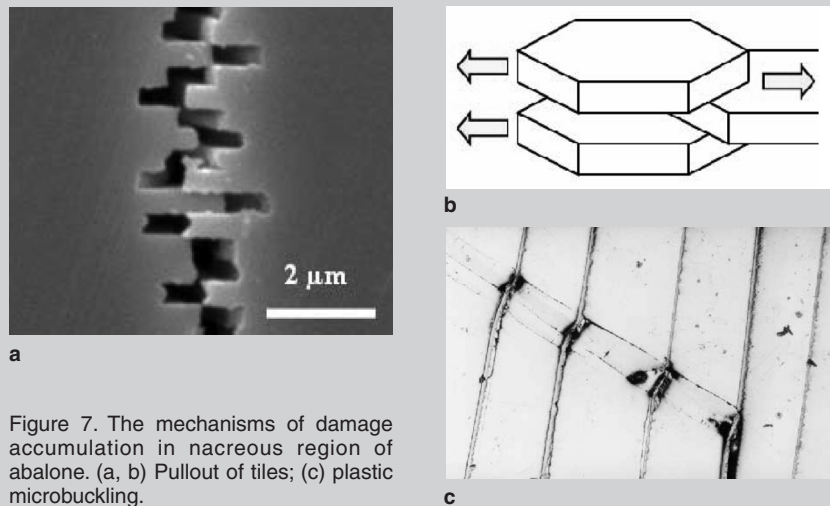


Figure 7. The mechanisms of damage accumulation in nacreous region of abalone. (a, b) Pullout of tiles; (c) plastic microbuckling.

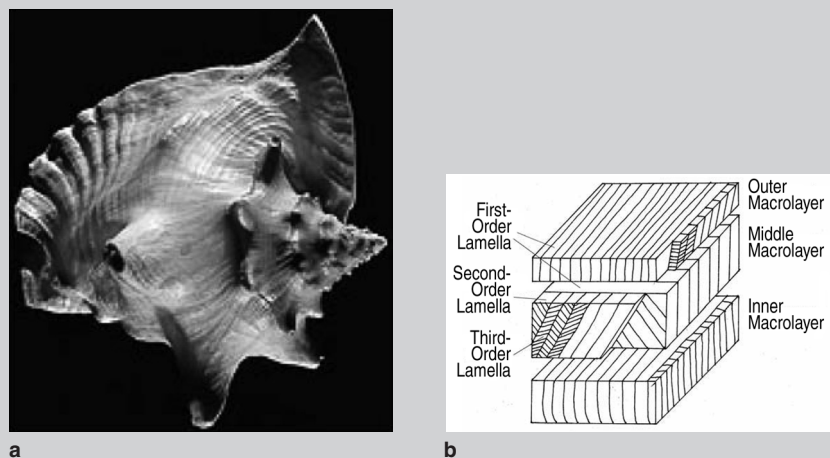


Figure 8. A conch shell: (a) overall view and (b) structure.

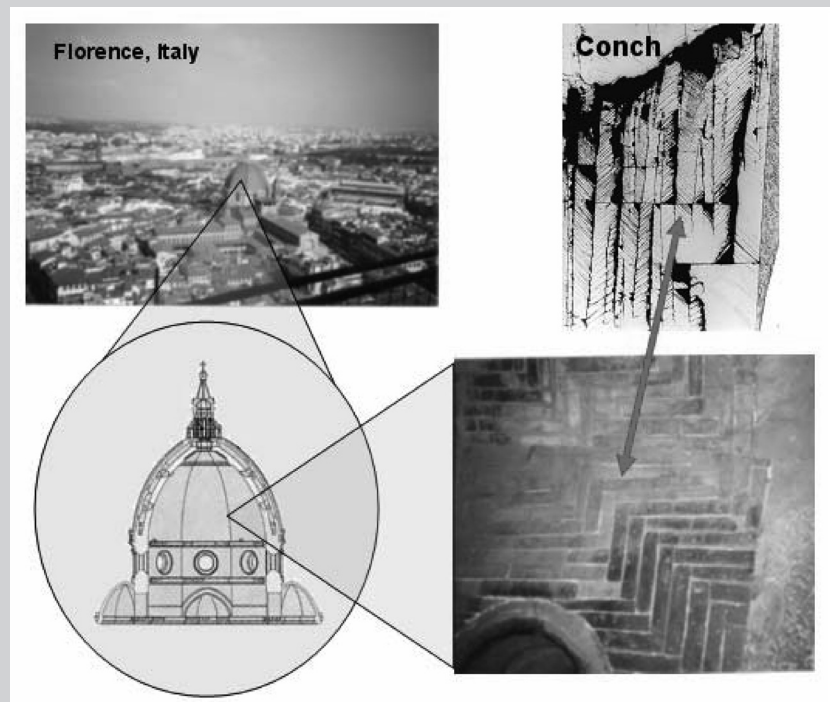


Figure 9. The tessellated bricks on Brunelleschi's Duomo (Florence, Italy) and equivalent structure of conch shell.

seen: plastic microbuckling. This mode of damage involves the formation of a region of sliding and of a knee. Figure 7c shows a plastic microbuckling event. The 5 wt.% of organic phase, the tensile significantly increased the strength, providing toughness to the shell.

The compressive strength of abalone is 1.5–3 times the tensile strength (as determined from flexural tests), in contrast with monolithic ceramics, for which the compressive strength is typically an order of magnitude greater than the tensile strength. The compressive strength, however, is not greatly altered

by the introduction

STROMBUS SHELL

The Strombus shells, which have a spiral configuration, have a structure that is quite different from the abalone nacre. Figure 8a shows the overall picture of the well known *Strombus gigas* (pink conch) shell. In contrast with the abalone shell, which is characterized by parallel layers of tiles, the structure of the conch consists of three macrolayers which are themselves organized into first-order lamellae, which are in their turn, comprised of second-order lamellae. These

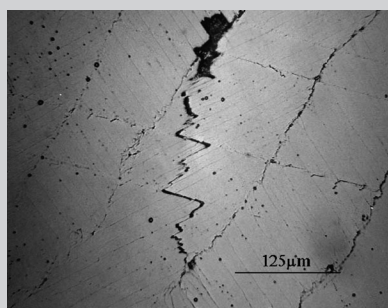
are made up of tiles in such a manner that successive layers are arranged in a tessellated (tweed) pattern. The three-tiered structure is shown in Figure 8b. This pattern, called cross-lamellar, is reminiscent of plywood or crossed-ply composites and has been studied extensively by Heuer and coworkers.^{18–20} An interesting analogy with a large dome structure is shown in Figure 9. The Florence dome, built by the architect Brunelleschi, uses a tessellated array of long bricks with a dimensional proportion similar to the tiles in conch. This arrangement provides the dome with structural integrity not possible before that time.

In conch, the fraction of organic material is lower than in abalone: ~1 wt.% vs. 5 wt.%. The strategy of toughening that is used in the conch shell is to delocalize cracking by distributing damage. An example of how a crack is deflected by the alternative layers is shown in Figure 10a. The fracture surface viewed by SEM shows the cross-lamellar structure (Figure 10b) in a clear fashion. The lines seen in the damaged surface of conch shown in Figure 9 indicate sliding of the individual, tiles. The absence of a clear crack leads to an increase in the fracture energy of 10,000 in comparison with monolithic calcium carbonate. The work of fracture is as high as 13 kJm.¹⁸

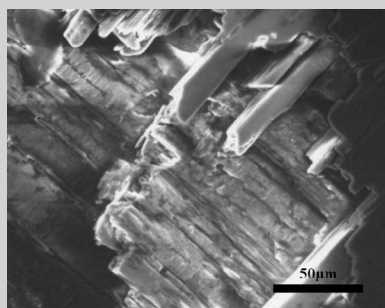
As in abalone, the ratio of the tensile strength to compressive strength is large in comparison to ceramics, providing increased toughness.

TOUCAN AND HORNBILL BEAKS

Beaks are fascinating structures that have received only scant attention from materials scientists. An exception is the study of the European starling by Bonser.^{21,22} The uniqueness of the toucan beak led to a recent study (Seki et al.¹¹), the results of which are summarized as follows. Beaks are usually short and thick or long and thin. The toucan beak is an exception; it is both long and thick. It comprises one third of the length of the toucan and yet only about 1/20th of its mass, while maintaining outstanding stiffness. The structure of a Toco toucan and hornbill beak, shown schematically in Figure 11, was found to be a sandwich composite with an exterior of keratin and a fibrous network of closed cells made of calcium-rich proteins. The

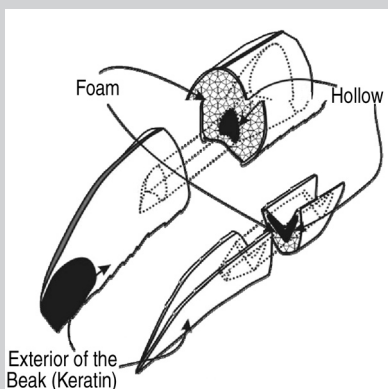


a

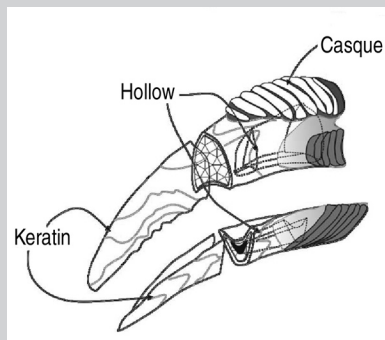


b

Figure 10. Fracture patterns in a conch shell; (a) crack delocalization shown in polished section and (b) scanning-electron micrograph of fracture surface showing cross lamellar structure.

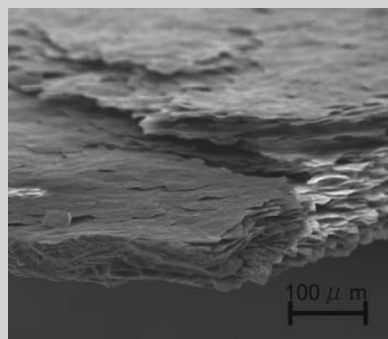


a

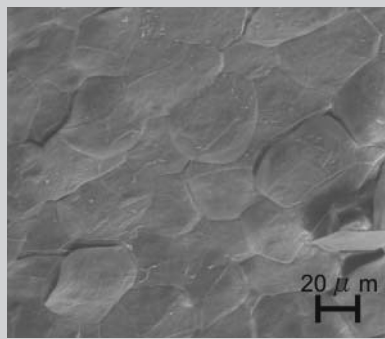


b

Figure 11. A schematic of the (a) toucan and (b) hornbill beaks.



a



b

Figure 12. A scanning-electron micrograph of exterior structure the beak keratin: (a) fracture region and (b) external surface.

keratin layer is comprised of superposed hexagonal scales (50 μm diameter and 1 μm thickness) glued together. This is shown in Figure 12. The interior of the beak is comprised of a cellular structure. Its density is on the order of 0.04 for the toucan and 0.14 for the hornbill. Figure 13 shows this foam at two magnifications. It is clear that it is comprised of webs and membranes and can therefore be considered a closed-cell foam as defined by Gibson and Ashby.²³ Thus, the overall density of the beak is approximately 0.1 for the toucan and 0.3 for the hornbill.

The tensile strength of the keratin is about 50 MPa and Young's modulus is 1.4 GPa (Figure 14a). The keratin shell exhibits a strain-rate sensitivity with a transition from slippage of the scales (due to release of the organic glue) at a low strain rate ($5 \times 10^{-5} \text{ s}^{-1}$) to fracture of the scales at a higher strain rate ($1.5 \times 10^{-3} \text{ s}^{-1}$). The closed-cell foam is comprised of fibers having a Young's modulus twice that of the keratin shells due to their higher calcium content. The compressive response of the foam, which is shown in Figure 14b, was successfully modeled by the Gibson-Ashby constitutive equation for closed-cell foam. The hornbill foam, which has a density three times higher than the toucan beak, has a strength that is correspondingly higher. There is a synergistic effect between foam and shell evidenced by experiments and analysis establishing the separate responses of shell, foam, and foam+shell. The stability analysis developed by Karam and Gibson,²⁴ assuming an idealized circular cross section, was applied to the beak. It shows that the foam stabilizes the deformation of the beak by providing an elastic foundation which increases its Brazier and buckling load under flexure loading.

CRAB EXOSKELETON

The exoskeleton of arthropods consists mainly of chitin. In the case of the lobster and crab, there is a high degree of mineralization. The structure of the sheep crab (*Loxorhynchus grandis*) claw is being studied in the authors' laboratories. It is similar to the structure of the lobster claw that was studied by Raabe et al.^{25,26} and consists of a complex network of highly mineralized chitin rods in a Bouligand²⁷ pattern interwoven with flexible fibers that stitch the structure

together. The hierarchy shown in Figure 3 is designed such that the structure has excellent mechanical properties. Figure 15 shows the lamellar structure in which each unit corresponds to a 180 degree rotation of the helix. A coordinate system

is shown on the side. The spacing in the external layer of exoskeleton (exocuticle) is approximately 3–5 μm , increasing to 10–15 μm in the inside layers (endocuticle). The Bouligand (helical stacking) arrangement provides structural strength

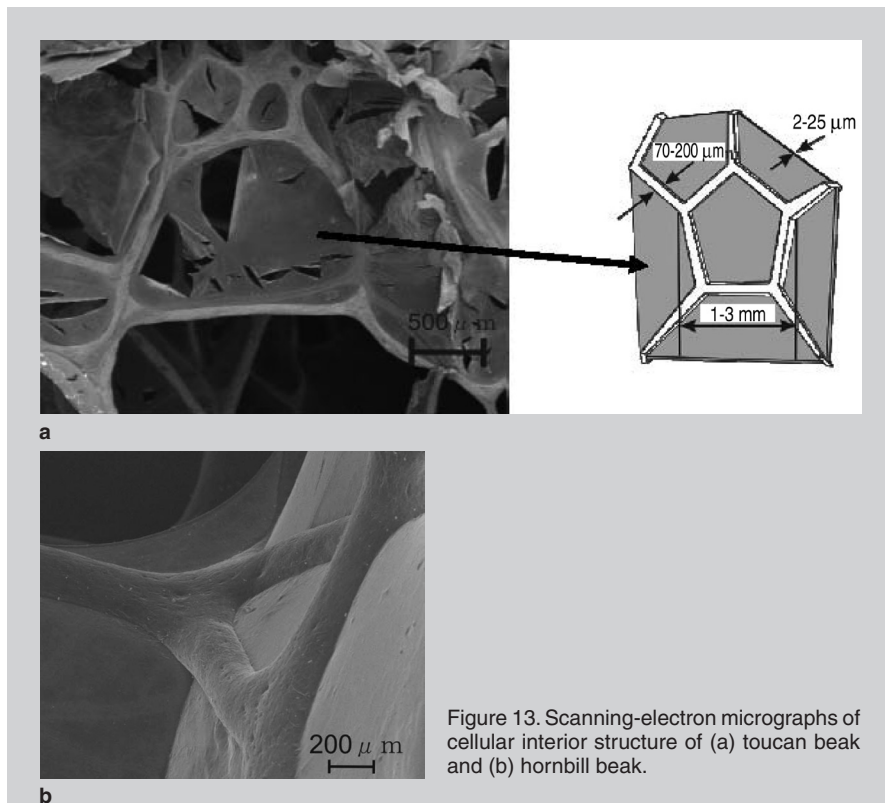


Figure 13. Scanning-electron micrographs of cellular interior structure of (a) toucan beak and (b) hornbill beak.

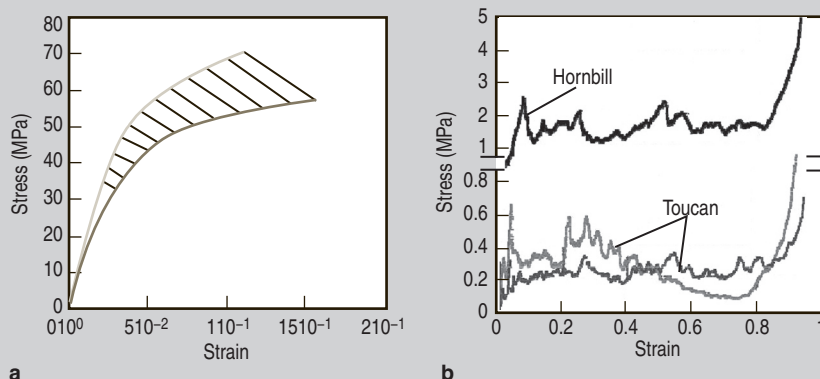


Figure 14. The mechanical properties of (a) keratin shell (tension) and (b) cellular bone interior (compression).

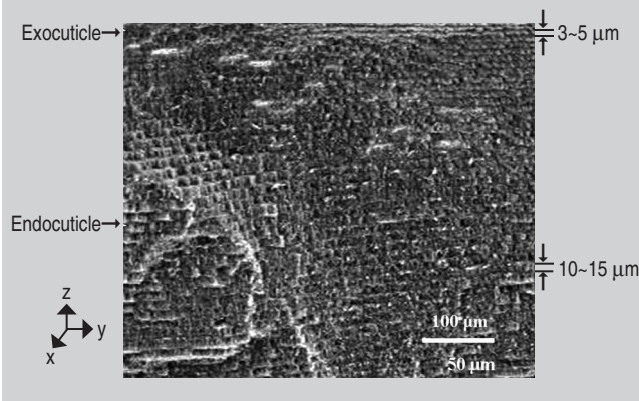


Figure 15. The parallel lines on fracture surface of crab exoskeleton evidencing periodic 180 degree rotations in Bouligand pattern.

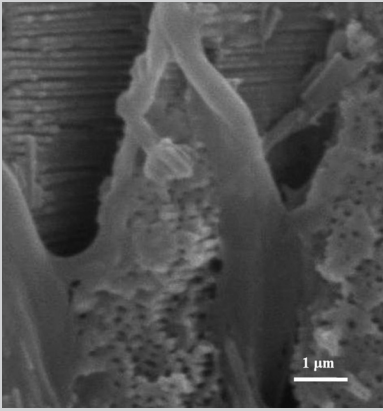


Fig 16. An SEM micrograph of fracture surface showing the twisted plywood (Bouligand) structure of crab exoskeleton.

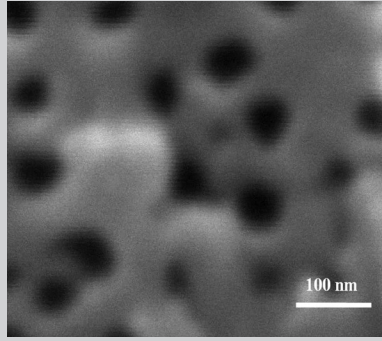


Figure 17. A detailed view of fracture section of brittle Bouligand component showing organic fibrils.

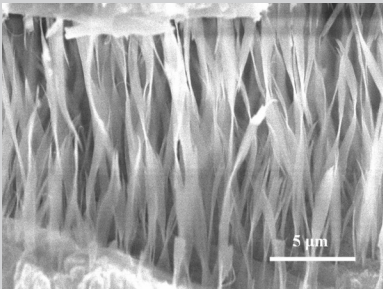
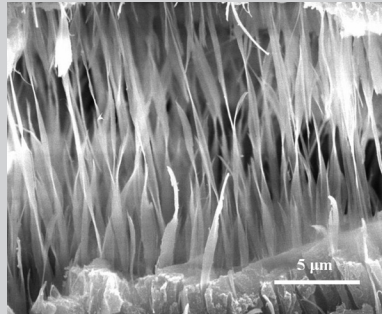


Figure 18. An SEM micrograph of fracture surface showing the tubules in the Z-direction in crab exoskeleton: (a) extended configuration and (b) necked configuration in tensile extension.



that is in-plane isotropic (plane XY) in spite of the anisotropic nature of the individual bundles

The fracture is brittle as is evident from the flat surfaces in Figure 16. There is a regular spacing of dark spots with diameters of approximately 50 nm. They are seen at higher magnification in Figure 17. These correspond to organic fibers, from which the mineral component grows. The spacing of these organic fibers is approximately 100 nm.

Canals enveloped in tubules are formed along the Z direction. These tubules are hollow and have a flattened configuration that twists in a helical fashion. A region where separation was introduced by tensile tractions is shown in Figure 18(a). The high density of these tubules (also schematically shown in Figure 3) is clearly evident. These tubules fail in a ductile mode as shown in Figure 18(b). The neck cross section is reduced to a small fraction of the original thickness (approximately 0.5–1 μm). It is thought that this ductile component helps to stitch together the brittle bundles arranged in the Bouligand

pattern and provides the toughness to the structure. It also undoubtedly plays a role in keeping the exoskeleton in place even when it is fractured, allowing for self healing. These aspects are currently under investigation.

CONCLUSIONS

Structural biological materials are complex composites that have structures that are being extensively investigated by materials scientists and engineers with the ultimate goal of mimicking them in synthetic systems. This is indeed a new frontier in materials science and is a fertile ground for innovative and far-reaching work. Although these composites have structures and constituent materials that vary widely, there is a commonality of architecture and properties:

- Synergism between brittle and ductile components in the structure
- Hierarchical organization
- Multifunctionality
- Ambient temperature processing; self assembly is one of the principal aspects of this process.²⁸
- Poor high-temperature performance

- Inherently weak (in comparison with synthetic materials) constituents. This can be clearly seen if one analyzes the mechanical performance maps developed by Ashby and Wegst²⁹ for biological materials.

ACKNOWLEDGEMENTS

This research is funded by the National Science Foundation Division of Materials Research, Ceramics Program (Grant DMR 0510138). We gratefully acknowledge support from Dr. Lynnette D. Madsen, program director. The help provided by Dr. Chris Orme, Lawrence Livermore National Laboratory, is greatly appreciated. The inspiration provided by Dr. George Mayer, University of Washington, is deeply appreciated, as well as the use of the nanoindentation facility by Professor Frank Talke, University of California at San Diego. Dr. M. Mace, Curator of Birds at the San Diego Zoo's Wild Animal Park, kindly provided us with hornbill beaks. Mr. Jerry Jenkins, owner of Emerald Forest Bird Gardens, has helped us immensely with the toucan beaks.

References

1. J.F.V. Vincent, *Structural Biomaterials* (Princeton, NJ: Princeton University Press, 1991).
2. A.V. Srinivasan et al., *Appl. Mech. Rev.*, 44 (1991), p. 463.
3. M. Sarikaya, *Microscopy Research and Technique*, 27 (1994), p. 360.
4. S. Mann, *Biomaterialization* (Oxford, U.K.: Oxford University Press, 2001).
5. G. Mayer, *Science*, 310 (2005), p. 1144.
6. G. Mayer et al., *MRS Symposium Proceedings, v. 844: Mechanical Properties of Bioinspired and Biological Materials*, ed. C. Viney et al. (Warrendale, PA: Materials Research Society, 2005), p. 79.
7. R. Menig et al., *Acta Mater.*, 48 (2000), p. 2383.
8. A. Lin and M.A. Meyers, *Mater. Sci. and Eng. A*, 390 (2005), p. 27.
9. A. Lin et al., *Mater. Sci. and Eng. C* (in press).
10. R. Menig et al., *Mater. Sci. and Eng. A*, 297 (2001), p. 203.
11. Y. Seki et al., *Acta Mater.*, 53 (2005), p. 5281.
12. Y. Seki et al., *Mater. Sci. and Eng. C* (in press).
13. P.-Y. Chen, A. Lin, and M.A. Meyers, unpublished results (2006).
14. C. Levi et al., *J. Mater. Sci. Lett.*, 8 (1989), p. 337.
15. J. Aizenberg et al., *Science*, 309 (2005), p. 275.
16. G. Mayer and M. Sarikaya, *Exper. Mech.*, 42 (2002), p. 395.
17. J.N. Cha et al., *Proc. Natl. Acad. Sci. USA*, 96 (1999), p. 361.
18. L.F. Kuhn-Spearing et al., *J. Mater. Sci.*, 31 (1996), p. 6583.
19. J.V. Loraia and A.H. Heuer, *J. Am. Ceram. Soc.*, 72 (1989), p. 2177.
20. A.H. Heuer et al., *Science*, 255 (1992), p. 1098.
21. R.H.C. Bonser, *J. Mater. Sci. Lett.*, 19 (2000), pp. 1039–1040.
22. *J. Mater. Sci. Lett.*, 21 (2002), p. 1563.

23. L. Gibson and M.F. Ashby, *Cellular Solids: Structure and Properties*, 2nd ed. (New York: Cambridge University Press, 1997).
24. G.N. Karam and L.J. Gibson, *Int. J. Solids Structures*, 32 (1995), pp. 1259, 1285.
25. D. Raabe et al., *Acta Mater.*, 53 (2005), p. 4281.
26. D. Raabe et al., *Mater. Sci. and Eng. A* (in press).
27. Y.J. Bouligand, *Tissue and Cell*, 4 (1972), p. 189.
28. G. Whitesides, *Mater. Res. Bulletin* (January 2002), p. 56. **[Couldn't find this listed in Jan. 2002 online to get volume or issue number.]**
29. M.F. Ashby and U.G.K. Wegst, *Phil. Mag.*, 84 (2004), p. 2167.

Marc A. Meyers, Albert Y.M. Lin, Yasuaki Seki, Po-Yu Chen, Bimal K. Kad, and Sara Bodde are with the Materials Science and Engineering Program in the Department of Mechanical and Aerospace Engineering at the University of California, San Diego.

For more information, contact Marc A. Meyers, University of California, San Diego, Materials Science and Engineering Program, Department of Mechanical and Aerospace Engineering, La Jolla, CA 92093; (858) 534-4719; fax (858) 534-5698; e-mail mameyers@ucsd.edu.